Percolation of intergranular fracture in Al-Li-Cu-Mg-Zr alloy during superplastic deformation: influence of grain boundary microstructure

Shigeaki Kobayashi[1,a], Sadahiro Tsurekawa[2,b] and Tadao Watanabe[3,c]

[1]Department of Mechanical Engineering, Faculty of Engineering, Ashikaga Institute of Technology, Omae-cho 268-1, Ashikaga, Tochigi 326-8558, Japan

[2]Faculty of Engineering, Kumamoto University, Kumamoto 860-8555, Japan

[3]Formerly Tohoku University, Sendai, Japan. Now Visiting Professor, Key Laboratory of Anisotropy and Texture of Materials, Northeastern University, Shenyang, PR China

[a]skoba@ashitech.ac.jp, [b]turekawa@kumamoto-u.ac.jp, [c]tywata@fk9.so-net,ne,jp

Keywords: Superplasticity; Intergranular fracture; Percolation; Grain boundary character distribution; Grain boundary connectivity; Triple junction distribution.

The effects of grain boundary microstructures, such as grain boundary character distribution (GBCD), grain boundary connectivity and triple junction distribution (TJD), on cavity nucleation and crack propagation in an Al-Li-Cu-Mg-Zr alloy during superplastic deformation have been investigated using the specimens with different grain boundary microstructures. The specimen having a homogeneous and fine grain structure with a high frequency of low-angle boundaries showed superplasticity, whereas the specimen having a heterogeneous duplex grain structure with a high frequency of random boundaries did not show superplasticity. In both types of specimens, low-angle boundaries changed into random boundaries during high temperature deformation, and these specimens fractured when the frequency of random boundaries increased to approximately 75% irrespective of the GBCD of initial microstructure. Cavities were preferentially nucleated at the triple junctions where more than two random boundaries interconnected. In addition, cracks propagated along random boundaries. Grain boundary microstructure that possesses a superior cavitation-resistance was suggested in terms of percolation of fracture-susceptible grain boundaries.

Introduction

Al-Li alloys are expected as structural materials for aircrafts because of their low density and high specific strength. However, workability of the Al-Li alloys is poor due to sever intergranular brittleness [1,2]. Superplasticity has a great potential to invest brittle polycrystalline materials like Al-Li alloys with well-workability. It is well known that grain boundary sliding dominantly promotes superplastic deformation of polycrystalline materials [3], and that the grain boundary sliding is strongly dependent on grain boundary character and structure [4,5]. Kokawa and Watanabe have found that the random boundaries can slide more easily than the coincidence site lattice (CSL) boundaries [4]. Moreover, accommodation of stress concentration at triple junctions due to grain boundary sliding is required to achieve superior superplasticity and to maintain soundness of post-deformed materials, because the stress concentration induces cavitation. Recently, we have found that cavities preferentially nucleated at triple junctions where more than two random boundaries interconnected, while cavitation hardly occurred at triple junctions composed of low-angle and CSL boundaries [6]. Therefore, control of grain boundary microstructures such as grain boundary character distribution (GBCD), grain boundary connectivity and triple junction distribution (TJD) was important for achieving enhanced resistance to intergranular fracture, and for development of large elongation.

In this work, the effect of initial grain boundary microstructures on the superplastic deformation has been investigated using two distinct specimens with different grain boundary microstructures. Cavity nucleation was studied in connection with change in grain boundary microstructure during superplastic

deformation. On the basis of these results, we suggested an optimal grain boundary microstructure for achieving enhanced resistance to cavitation and to percolation of fracture susceptive boundaries.

Experimental procedure

Specimen preparation. The material used in this study was an Al-2.2Li-2.5Cu-1.2Mg-0.15Zr (in mass%) alloy , which was subjected to hot rolling to 80% strain at 723K, solution treatment at 803K for 7.2ks, aging at 673K for 115.2ks, and finally to cold rolling to 85% strain. Tensile specimens with 10mm long, 4mm wide and 1mm thick were cut using a spark machine. The tensile direction was parallel to the rolling direction. Thereafter, these specimens were subjected to different two annealing processes in order to obtain different grain boundary microstructure. Specimens as Type A and Type B were annealed at 723K for 7.2ks, and at 793K for 10.8ks, respectively, in an Ar atmosphere. Finally, they were annealed at 673K for 21.6ks in an Ar atmosphere in order to stabilize particles precipitated.

Evaluation of grain boundary microstructures. The automated FE-SEM/EBSD/OIM (orientation imaging microscopy) [7] was applied to quantitatively analyze grain boundary microstructure in pre- and post-deformed specimens. Electron beam was scanned with a 0.7μm step size over an area of 60μm×60μm at an accelerated voltage of 30kV.

In this work, grain boundaries with $\Sigma \leq 29$ were defined as CSL boundaries with an allowable angular deviation given by the Brandon's criterion, $\Delta\theta = 15/\Sigma^{1/2}$ (in degree) [8]. The low-angle boundaries ($\Sigma 1$ boundaries) were differently considered from other CSL boundaries, because the frequency of low-angle boundaries was significantly high.

High-temperature tensile tests. Tensile tests were carried out at 723K and at initial strain rates of $1.0\times10^{-4}s^{-1}$ - $5.0\times10^{-3}s^{-1}$ in air using a Shimadzu Autograph (AG-50kNG model) with a split type of electric furnace. Tensile tests were interrupted at different strains in order to observe the grain boundary microstructure at different stages of superplastic deformation. To freeze the microstructure during deformation, the specimen deformed up to a predetermined strain was rapidly cooled down to room temperature within 120s by blowing cold air in unloading condition.

Results and discussions

High temperature deformation behavior of Al-Li alloy with different initial microstructure. Figures 1 (a) and (b) show true stress - true strain curves for Type A and Type B specimens, respectively, deformed at 723K at an initial strain rates between 1.0×10^{-4} s^{-1} and 5.0×10^{-3} s^{-1}. Microstructure of the specimens evaluated using an OIM were also shown in this figure. The Type A specimen possessed a homogeneous fine-grained structure with the average grain size of 4μm, in which the grain orientation distributed between <110> and <112> orientation. The frequency of low-angle boundaries was as high as 55%. On the other hand, the Type B specimen possessed a heterogeneous duplex grain structure composed of fine grains of 9μm grain size and coarse grains of 23μm, and the grain orientation was randomly distributed. The frequency of low-angle boundaries in Type B specimen was 27%. The frequency of low-angle boundaries in Type B specimen was lower than that in Type A specimen. Conversely, the frequency of random boundaries was high (63%) in Type B specimen.

Flow stress in Type A specimen increased with increasing strain rate. Deformation tended to go into steady state following the work softening regime when the strain rate was less than 5×10^{-4} s^{-1}. The maximum true strain of 1.25 (253% in elongation) was obtained at a strain rate of 2.5×10^{-4} s^{-1}. Conversely, the strain was decreased with further decrease in strain rate.

The flow stresses were higher for Type B specimen than for Type A specimen. The true stress – true strain curves showed a high work-hardening rate after yielding, which is characteristic feature of

dispersion strengthened alloys [9]. The flow stress decreased monotonically after showing a peak in the stress. Type B specimens did not show superplasticity at any strain rates. These specimens fractured at a small strain of less than 0.65 (91% in elongation).

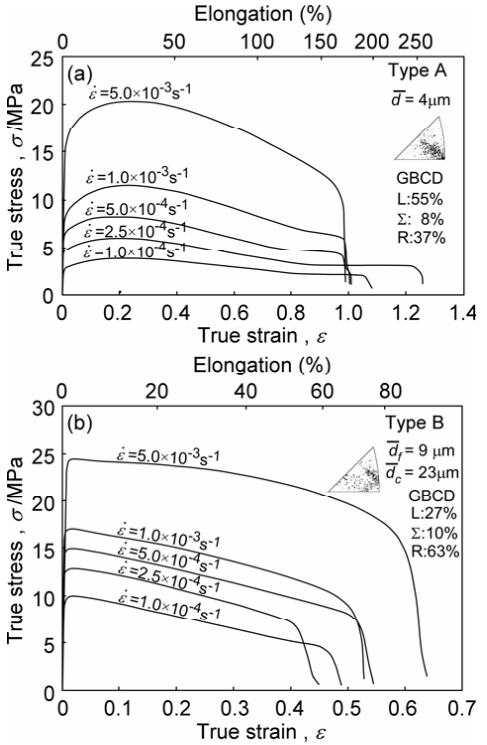

Figure 1 True stress - true strain curves for (a) Type A and (b) Type B specimens deformed at 723K at various strain rate.

Change in grain boundary microstructure during high temperature deformation. Figure 2 (a) and (b) show changes in GBCD with high temperature deformation of Type A and Type B specimens, respectively, deformed at 723K and at a strain rate of 2.5×10^{-4} s^{-1}. The GBCD was evaluated on the specimen surface rolled. Figure 2 (a) reveals that the GBCD did not change significantly until the flow stress approach a peak stress (R: 37% - 41%). In this regime, the average grain size and the grain orientation distribution were less-dependent on deformation. However, OIM analyses revealed that a high density of dislocations were introduced into the grain interior at the deformation stage ranging from (ii) to (iii) displayed in the figure. Thereafter, the dislocation density was decreased at the work softening stage, probably because of deformation-induced continuous recrystallization, and the average grain size was slightly increased. Dislocations introduced at the stage between (ii) and (iii) would act as a driving force for grain boundary migration (grain growth) at the work softening stage (iv). In addition, it is interesting to note that some low-angle boundaries appear to change into high-angle random boundaries by absorbing dislocations in grain interior. The frequency of random boundaries increased successively from 37% to 72% in the work softening regime (Fig. 2 (a) (iii)-(v)). As the result, grain boundary sliding may have been enhanced, and then superplastic deformation occurred at the steady state regime.

The frequency of random boundary in Type B specimen was increased from 63% to 73% during the high temperature deformation to fracture. Although Type B specimens had a duplex grain structure composed of fine-grained and coarse-grained structures, their grain structure was changed into homogeneous one with the average grain size of 25μm during deformation.

The frequencies of random boundaries were 72%-75% irrespective of initial grain boundary microstructure when the specimens fractured. In the following section, the relationship between grain boundary microstructures and cavitation will be discussed.

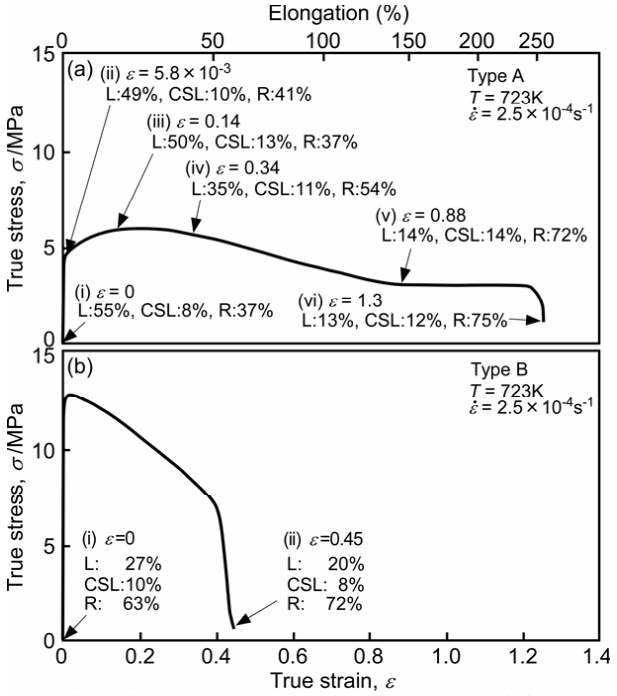

Figure 2 Change of grain boundary microstructures in (a) Type A and (b) Type B specimens during high temperature deformation at 723K at strain rate of 2.5×10^{-4} s^{-1}.

Cavity nucleation and growth during high temperature deformation. Figure 3 (a) and (b) are a SEM micrograph and an illustration, respectively, of the surface of Type A specimen deformed to 253% elongation at 723K and at 2.5×10^{-4} s^{-1}, showing cavity formation at triple junctions. The characters of individual grain boundaries determined with the OIM are shown in Fig. 3 (b). It is found that most cavities nucleated at triple junctions and grew along grain boundaries. In particular, the triple junctions where more than two random boundaries interconnected, such as L-R-R (R2), Σ-R-R (R2) and R-R-R (R3), are found to act as effective nucleation sites for cavitation, and then the cavities grow along random boundaries. The fraction of cavitation at R3 and R2 junctions were 57% and 37%, respectively, while the fraction of cavitation at R0 (with no random boundary at triple junction) and R1 (with 1 random boundary) junctions were 0% and 14%, respectively.

Figure 4 shows the change in the relative density of the Type A specimen during deformation. The density of specimens was measured by the Archimedes method. In this figure, the frequency of susceptible triple junctions (R2 and R3 type) was also shown to reveal the relationship between the triple junction character distribution and cavitation during superplastic deformation. The relative density slightly decreased until the beginning of work-softening stage. However, it observably

decreased from 97.8% to 90.8% at this stage. It is interesting to see that the decrease in relative density is coincident with the increase in cavitation susceptible triple junctions (R2 and R3). Therefore, control of frequency and connectivity of random boundaries is great importance to develop superplasticity and to prevent cavitation in polycrystalline materials.

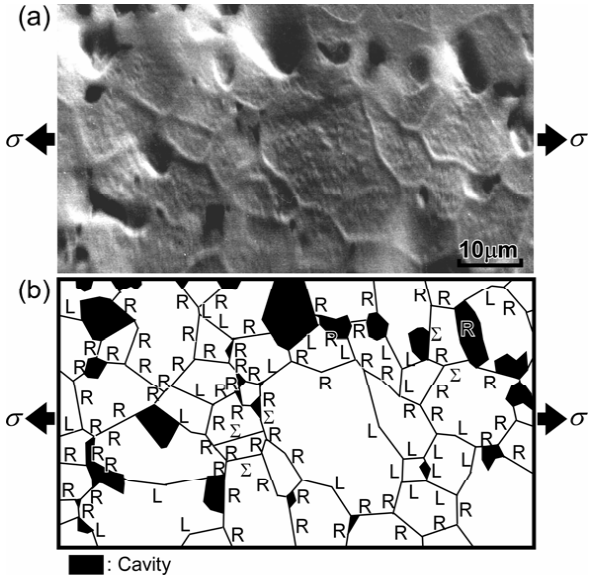

Figure 3 Cavity nucleation and growth at triple junctions in post-deformed Type A specimen.

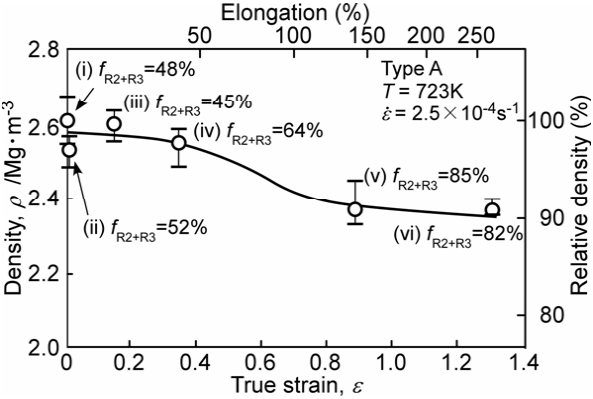

Figure 4 Change in the relative density of the Type A specimen during superplastic deformation.

Grain boundary engineering for improvement in superplasticity. Control of cavitation is important for development of superplasticity and soundness of post-deformed materials. It is considered that the optimization of the frequency and connectivity of random boundaries is essential for improvement in superplasticity.

Figure 5 shows the relationship between the frequency of percolation-resistant triple junctions and the total frequency of low-angle and CSL boundaries (special boundaries) in Type A and Type B specimens during deformation at 723K and at 2.5×10^{-4} s^{-1}. Following Kumar et al. [10], the frequency of resistant triple junctions to intergranular degradation like crack propagation was defined as f_{R1}/(1-

f_{R0}) in order to evaluate the continuity of percolation paths in the polycrystalline materials. The data for fcc materials with a low-stacking fault energy like Inconel 600 [10], copper [10], SUS304L [11] and bcc molybdenum [12] are included in this figure. The frequency of resistant triple junctions in Type A and Type B specimens are found to increase with increasing frequency of special boundaries according to a common curve within a experimental error. The result observed in the present work is in good agreement with previous work for fcc materials with a low stacking fault energy and bcc molybdenum with a high stacking fault energy. It can be concluded that the percolation-resistant triple junction distribution is predominantly governed by the frequency of special boundaries or random boundaries. According to Kumar et al. [10], the percolation pass in microstructure is broken when the frequency of resistant triple junctions is more than 35%. The type A specimen maintained the frequency of approximately 30% until the beginning of work-softening stage. On the other hand, the Type B specimen had a lower frequency of less than 20% even in the initial microstructure.. Therefore, percolation of intergranular crack along the random boundaries would be more pronounced in Type B specimen than in Type A specimen, which is a possible reason for premature failure in Type B specimen.

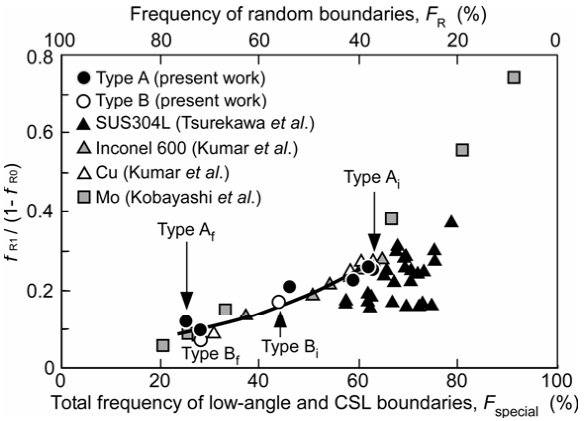

Figure 5 Change in frequency of percolation-resistant triple junction as a function of total frequency of low-angle and CSL boundaries for the Type A and Type B specimens.

Figure 6 shows the percolation probability of random boundaries, which act as a preferential pass for intergranular fracture, as a function of total frequency of low-angle and CSL boundaries for Type A and Type B specimens. Following the bond process of percolation theory [14], the percolation probability was determined from the ratio of the number of random boundaries in the largest radom boundary cluster to the total number of all grain boundaries. The percolation probability decreases with increasing frequency of special boundaries. The percolation threshold is found to occur at the frequency of approximately 60% special boundaries. This threshold value for percolation is slightly smaller than those based on the boundary length for SUS304L [11] and SUS316 [13]. According to Frary and Schuh [14], the 2D percolation threshold in general textured grain boundary network taking account of Σ-product rule is about 66%. The threshold value for percolation based on 2D OIM data in this work agrees with the value of 2D grain boundary network.

From these results, the percolation of intergranular fracture which follows cavitation at triple junctions can be controlled by decreasing frequency of random boundaries. Since the grain boundary sliding which promotes superplastic deformation should be accelerated by increasing frequency of random boundaries, the superplastic elongation and the soundness of post-deformed material can be improved by optimizing grain boundary microstructure. Actually, we demonstrated that the

superplastic elongation could be improved by modifying grain boundary microstructure by application of strain rate change tests at the work softening stage [6].

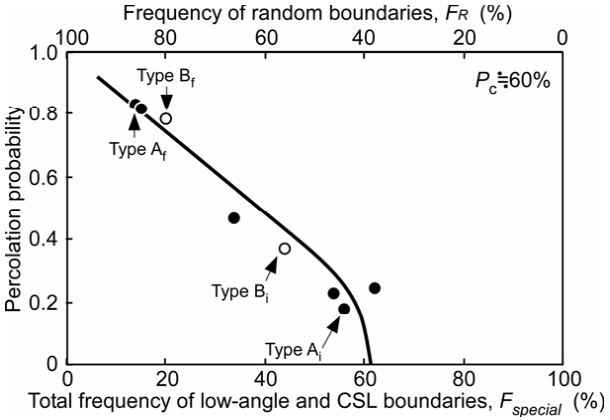

Figure 6 Percolation probability as a function of total frequency of low-angle and CSL boundaries for Type A and Type B specimens during high temperature deformation.

Conclusions

Cavity nucleation and percolation of intergranular fracture during superplastic deformation was assessed in connection with grain boundary microstructure using two distinct Al-Li-Cu-Mg-Zr alloy samples with different microstructure. The main results obtained are as follows.

(1) The specimen having a homogeneous fine grain structure with a high frequency of low-angle boundaries showed superplasticity (Type A), whereas the specimen having a heterogeneous duplex grain structure with a high frequency of random boundaries did not show superplasticity (Type B).

(2) Low-angle boundaries changed into random boundaries during high temperature deformation, and both types of specimens fractured when the frequency of random boundaries approached 75% irrespective of the GBCD of initial specimens.

(3) Cavities were preferentially nucleated at the triple junctions where more than two random boundaries interconnected, and cracks propagated along random boundaries.

(4) The percolation of intergranular fracture could be prevented by increasing the frequency of special boundaries to more than 60%.

Acknowledgements

The authors would like to express their hearty thanks to Professor Jianzhang Cui of Northeastern University, China for the supply of Al-Li-Cu-Mg-Zr alloy sheet.

References

[1] F.S. Lin, S.B. Chakrabortty and E.A. Starke, Jr.: Metall. Trans. Vol. 13A (1982), p. 401

[2] D. Dew-Hughes, E. Creed and W.S. Miller: Mater. Sci. Tech. Vol. 4 (1988), p. 106

[3] D.M.R. Taplin, G.L. Dunlop and T.G. Langdon: Ann. Rev. Mater. Sci. Vol. 9 (1979), p. 151

[4] H. Kokawa, T. Watanabe and S. Karashima: Phil. Mag. Vol. A44 (1981), p. 1239

[5] T. Watanabe, S. Kimura and S. Karashima: Phil. Mag. Vol. A49 (1984), p. 845

[6] S. Kobayashi, T. Yoshimura, S. Tsurekawa, T. Watanabe and J-Z. Cui: Mater. Trans. Vol.44 (2003), p. 1469

[7] B.L. Adams, S.I. Wright and K. Kunze: Metall. Trans. Vol. 24A (1993), p. 819

[8] D.G. Brandon: Acta Metall. Vol. 14 (1966), p. 1479

[9] A.M. Hammad and K.K. Ramadan: Z. Metallkde. Vol. 80 (1989), p.178

[10] M. Kumar, W.E. King and A.J. Schwartz: Acta Mater. Vol. 48 (2000), p. 2081

[11] S. Tsurekawa, S. Nakamichi and T. Watanabe: Acta Mater. Vol. 54 (2006), p. 3617

[12] S. Kobayashi, S. Tsurekawa, T. Watanabe and A. Kobylanski: Phil. Mag. Vol. 88 (2008), p. 489

[13] M. Michiuchi, H. Kokawa, Z.J. Wang, Y. S. Sato and K. Sakai: Acta Mater. Vol. 54 (2006), p. 5179

[14] M. Frary and C.A. Schuh: Phil. Mag. Vol. 85 (2005), p. 1123